Clustering and Mechanics in Dense Depletion and Thermal Gels†

S. Ramakrishnan, V. Gopalakrishnan, and C. F. Zukoski*

Department of Chemical and Biomolecular Engineering, University of Illinois at Urbana-Champaign, Urbana, Illinois 61801

Received March 29, 2005. In Final Form: June 13, 2005

We report on the microstructure and mechanical properties (elastic modulus) of concentrated depletion and thermal gels of octadecyl-coated silica particles for different values of the strength of interaction—polymer concentration for depletion gels and temperature for thermal gels. The depletion gels are composed of dense clusters and voids, while the thermal gels are devoid of clusters. Shear breaks up clusters in depletion gels while it induces clustering in the thermal gels. In both of these gels, the microstructure recovers to the presheared state upon cessation of shear. The recovery of the elastic modulus mimics the microstructure in the sense that the elastic modulus recovers to the presheared sheared state after shearing is stopped. Calculations of the gel boundary by modeling the interactions with an effective one-component square-well model reveals that suspensions with similar ranges of attraction gel at the same volume fraction at a fixed strength of attraction. Calculations of the elastic modulus using the naïve mode coupling theory for depletion gels are in good agreement with experimental measurements provided clustering is taken into account and have the same magnitude as the elastic moduli of thermal gels with similar strengths of attraction. These calculations, in addition to the experimental observations reinforce the point that the microscopic parameter determining the elastic modulus of dense gels and its recovery is the localization length which is only a fraction of the particle diameter and not the structure on the length scale of the particle diameter and larger.

1. Introduction

Due to their unique flow properties, colloidal gels are used in a wide variety of applications—such as processing of ceramics, coatings, inks, personal care products, and minerals processing.[1] These materials are composed of suspensions of micrometer- and submicrometer-sized particles that have elastic moduli, G', that are weakly dependent upon frequency and apparent yield stresses, τ_y, both of which increase with particle volume fraction, ϕ[2]. Deformation results in flow, but in the absence of shear, solidlike behavior is recovered. An approach commonly followed to predict gel flow properties starts by inferring a specific particle interaction energy and gel microstructure. Progress toward general models for gel properties requires an understanding of what microstructures occur within gels and how these vary with type of interaction and process history.

A microstructural model for colloidal gels commonly used in prediction of G' and τ_y far from the gelation threshold is based on arguments that the gels have a fractal microstructure.[3−6] For example, the approach of Aksay and co-workers[3,4] developed for dilute gels predicts that the power law exponents relating G' to ϕ are set by the gel's microstructure. In their approach, elastic moduli are related to bond elasticities that are held constant while the number of bonds per particle or aggregate is related to volume fraction through the self-similar properties of fractal materials.

Power law dependencies of modulus and yield stress on ϕ are also observed in dense colloidal and nanoparticle gels.[7−12] For example, the elastic modulus of gels composed of octadecyl silica particles suspended in hexadecane display forms of $G' \approx \phi^x$ where the exponent depends on the strength of attraction. Rueb and Zukoski[12] extended the work of Grant and Russel[7] and studied the rheological properties of dense octadecyl silica particles suspended in decalin over a wide range of temperatures and volume fractions ($0.15 < \phi < 0.55$). In a similar way, power law exponents are observed in dense depletion gels produced by addition of nonadsorbing polymer to nanoparticle suspensions.[13] Commonly in dense colloidal gels, the exponent x lies between 5 and 8. In these dense systems, concepts of a fractal microstructure are of limited applicability, as the size of a fractal cluster rapidly becomes on the order of a single particle thus suggesting that a different approach is warranted.

Detailed studies on dense depletion gels show that they are composed of dense interpenetrating clusters.[13] Studies on the elastic properties of these materials are thus made on a composite of aggregates and non-stress-bearing fluid. The origin of these clusters and their impact on mechanical properties remains poorly understood. One hypothesis is that the clusters are produced in the mixing process involved in the gel. The microstructure of concentrated suspensions at rest and under flow has been studied by neutron scattering experiments.[12,14,15] Neutron scattering

† Part of the Bob Rowell Festschrift special issue.

* To whom correspondence should be addressed. E-mail: czukoski@uiuc.edu.

(1) Lewis, J. A. *J. Am. Ceram. Soc.* **2000**, *83*, 2341.
(2) Russel, W. B.; Saville, D. A.; Schowalter, W. R. *Colloidal Dispersions*; Cambridge University Press: Cambridge, 1989.
(3) Shih, W. H.; Shih, W. Y.; Kim, S. I.; Liu, J.; Aksay, I. A. *Phys. Rev. A* **1990**, *42*, 4772.
(4) Shih, W. Y.; Shih, W. H.; Aksay, I. A. *J. Am. Ceram. Soc.* **1999**, *82*, 616.
(5) Potanin, A. A.; Derooij, R.; Vandenende, D.; Mellema, J. *J. Chem. Phys.* **1995**, *102*, 5845.
(6) Trappe, V.; Weitz, D. A. *Phys. Rev. Lett.* **2000**, *85*, 449.
(7) Grant, M. C.; Russel, W. B. *Phys. Rev. E* **1993**, *47*, 2606.
(8) Channell, G. M.; Zukoski, C. F. *AIChE J.* **1997**, *43*, 1700.
(9) Buscall, R.; McGowan, I. J.; Mills, P. D. A.; Stewart, R. F.; Sutton, D.; White, L. R.; Yates, G. E. *J. Non-Newtonian Fluid Mech.* **1987**, *24*, 183.
(10) Buscall, R.; Mills, P. D. A.; Goodwin, J. W.; Lawson, D. W. *J. Chem. Soc., Faraday Trans.* **1988**, *84*, 4249.
(11) Yanez, J. A.; Laarz, E.; Bergstrom, L. *J. Colloid Interface Sci.* **1999**, *209*, 162.
(12) Rueb, C. J.; Zukoski, C. F. *J. Rheol.* **1997**, *41*, 197.
(13) Ramakrishnan, S.; Chen, Y. L.; Schweizer, K. S.; Zukoski, C. F. *Phys. Rev. E* **2004**, *70*, 040401(R).
(14) Maranzano, B. J.; Wagner, N. J. *J. Chem. Phys.* **2002**, *117*, 10291.

10.1021/la050830w CCC: $30.25
Published on Web 08/09/2005

experiments on sheared organophilic silica−tetradecane gels[12] shows that the fractal dimension can increase with shear rate, suggesting the densification of floc structure with shear. Upon cessation of shear, structures can be frozen and not return to rest states, thus affecting the recovery of mechanical properties of the gel. In dilute gels, Varadan and Solomon[16] demonstrated that shear produced clusters with size increasing with shear rate.

Despite different microstructures, the systems studied have similar dependencies on ϕ, suggesting that linear and nonlinear properties are weakly coupled to the microstructure as measured on the length scale of a particle diameter or larger. This observation can be rationalized within the context of recently developed mode coupling theory (MCT) discussions of the origins of gelation.[17,18] MCT attempts to capture the highly cooperative nature of particle interactions that result in nonergodic states. Originally developed and applied to glass formation and verified for colloidal hard sphere glass formation, the theory has been extended to attractive systems where the gel boundary can be predicted as a function of strength and range of interparticle attraction and volume fraction.[19,20] A recently developed extension of mode coupling theory, naïve mode coupling theory (NMCT) provides a facile method to approximate the predictions of the full mode coupling approach.[21] Within the context of mode coupling theories, at the gel point, the particles are localized and cannot diffuse over distances large compared to a particle diameter.

Starting from the equations of motion, the NMCT approach develops an expression for the localization length or maximum root-mean-square diffusive displacement of the particle r_{loc}^2. Given r_{loc} and the structure factors, the zero-frequency elastic modulus follows from the standard Green-Kubo formula plus the MCT factorization.[13,22] The characteristic elasticity is given by $\phi kT/r_{loc}^2$, which can be thought of as an "effective spring constant" of an elastic network. As one moves deeper into the gel (by increasing ϕ or the strength of attraction), r_{loc} shrinks with the result being that G' increases. NMCT is thus capable of predicting both the location of the gel boundary and the mechanical properties of the gel within one model. The input into NMCT is the equilibrium structure factor for the suspension, and thus NMCT can be applied to dilute and dense colloidal gels. In addition, as opposed to long-range structures governing mechanical properties as is proposed in fractal models of dilute gels, NMCT predicts that the important length scale is r_{loc}, which is typically a small fraction of a particle diameter. This suggests that structures on the length scale of a particle diameter and larger do not dominate the onset of nonergodic behavior and have a weak influence on the gel's mechanical properties.

NMCT has been applied to dense colloidal gels where the particle attraction is developed by the addition of nonadsorbing polymer to hard sphere particles.[13,23] The polymer concentration and volume fraction dependencies of the gel boundary and elastic moduli are well captured by the NMCT predictions.[13,23] The absolute magnitude of the predictions of gel modulus differs from the measured values by a nearly constant factor. This factor is closely related to the observations that the depletion gels consist of dense interpenetrating clusters where the characteristic cluster size is measured to be $\xi \approx 3-5D$, where D is the particle diameter. Using a simple ansatz that the macroscopic properties of these depletion gels arise from those of a composite consisting of dense clusters and nonelastic voids, remarkable quantitative agreement is achieved between the modulus predictions of NMCT, G'_{NMCT}, and experimental measurements, G' when $G' = G'_{NMCT}(D/\xi)$.[3]

These successes are predicated on having a model for the equilibrium structure factor, $S(q)$, for depletion systems. In the studies described above, the polymer reference site interaction model (PRISM) for $S(q)$ was used to describe the thermodynamics of the colloid−polymer system.[24,25] Previous detailed studies indicate that PRISM predictions capture subtle variations in $S(q)$ with changes in volume fraction and polymer concentration in equilibrium fluids.[26,27] Application of this model to the gelled state indicates that G'_{NMCT} is weakly dependent on $S(q)$ for $qD < 6$ and is dominated by the behavior of $S(q)$ at $q \approx 2\pi/r_{loc}$. The presence of clusters acts to modulate this qualitative behavior by creating a composite, but these clusters have no impact on r_{loc} and thus the characteristic gel modulus.

The clusters measured in depletion gels have characteristic lengths that are weakly dependent on polymer concentration (strength of attraction) and volume fraction. Here we investigate if such clusters are a common feature of dense gels and if clusters are always formed by shearing a gel. We do this by investigating the effect of shear on the microstructure of depletion and thermal gels. Both systems are composed of octadecyl silica particles suspended in decalin. In the former case, polystyrene is added to induce a depletion gel, while in the thermal gels, gelation is induced by lowering the temperature. For thermal gels, we investigate the microstructure in the quenched and sheared states. Our results suggest that not all gels have the same microstructure and that, while shear alters the microstructure, both types of gel recover to the presheared microstructure upon cessation of shear. Finally, we show that the NMCT predictions of the depletion gel moduli capture the magnitude of the moduli of thermal gels where particles experience a similar strength and range of attraction.

Below in Section 2, we describe our experimental systems where we use octadecyl silica particles to produce both thermal and depletion gels. These systems are chosen such that the range of attraction is approximately the same, providing the opportunity to compare mechanical properties at equal strengths of attraction. In Section 3, we discuss the gel boundary and use the MCT-based model of Fuchs and Bergenholtz[19,20] to relate polymer concentration and temperature to the strength of attraction. We follow with experimental evidence that depletion and thermal gels have fundamentally different microstructures on length scales of a particle diameter and larger. We provide evidence that the clusters seen in the depletion gels are broken by deformation while shear produces clusters in thermal gels. In both cases, upon cessation of shear, the gels recover to the presheared state. We close

(15) Chen, L. B.; Ackerson, B. J.; Zukoski, C. F. *J. Rheol.* **1994**, *38*, 193.
(16) Varadan, P.; Solomon, M. J. *Langmuir* **2001**, *17*, 2918.
(17) Gotze, W.; Sjogren, L. *Rep. Prog. Phys.* **1992**, *55*, 241.
(18) Bengtzelius, U.; Gotze, W.; Sjolander, A. *J. Phys. C: Solid State* **1984**, *17*, 5915.
(19) Bergenholtz, J.; Fuchs, M. *J. Phys.: Condens. Matter* **1999**, *11*, 10171.
(20) Bergenholtz, J.; Fuchs, M. *Phys. Rev. E* **1999**, *59*, 5706.
(21) Schweizer, K. S.; Saltzman, E. J. *J. Chem. Phys.* **2003**, *119*, 1181.
(22) Chen, Y. L.; Schweizer, K. S. *J. Chem. Phys.* **2004**, *120*, 7212.
(23) Shah, S. A.; Chen, Y. L.; Schweizer, K. S.; Zukoski, C. F. *J. Chem. Phys.* **2003**, *119*, 8747.
(24) Fuchs, M.; Schweizer, K. S. *Phys. Rev. E* **2001**, *6402*.
(25) Fuchs, M.; Schweizer, K. S. *J. Phys.: Condens. Matter* **2002**, *14*, R239.
(26) Shah, S. A.; Chen, Y. L.; Ramakrishnan, S.; Schweizer, K. S.; Zukoski, C. F. *J. Phys.: Condens.* Matter **2003**, *15*, 4751.
(27) Shah, S. A.; Ramakrishnan, S.; Chen, Y. L.; Schweizer, K. S.; Zukoski, C. F. *Langmuir* **2003**, *19*, 5128.

Section 3 with a comparison of the modulus of depletion and thermal gels at the same strengths of attraction where we show that depletion gels have substantially smaller moduli and that the detailed NMCT calculations carried out for the depletion gels capture the magnitude of the thermal gels with no adjustments for clustering. In Section 4, we draw conclusions.

2. Experimental Section

Silica particles ($D = 90 \pm 6$ nm) were prepared by the base-catalyzed hydrolysis and condensation of tetraethyl orthosilicate according to the method of Stober, Fink, and Bohn,[28] and a seeded growth technique of Bogush and Zukoski[29] to increase the particle diameter. The particles were then rendered hydrophobic via the method of van Helden, Jansen, and Vrij[30] and characterized with electron microscopy, ultra-small-angle X-ray scattering, and dynamic light scattering. The synthesized particles had a gravimetrically determined density of $\rho_c = 1.9 \pm 0.04$ g/mL. Suspensions were prepared by dispersing a known mass of dried silica powder in a 50:50 mixture of cis- and trans-decalin followed by stirring to better disperse the powder. The volume fractions were also determined by dry weight using $\phi = c/\rho_c$, where c is the mass concentration (g/mL) of the silica in suspension. In the absence of added polymer, octadecyl silica spheres suspended in decalin are model hard spheres. Polystyrene of molecular weight 18 700 g/mol was purchased from Aldrich Chemical Co. The ratio of the weight average to number average molecular weight is 1.03, implying monodisperse samples. Polymer characterization has been previously reported where decalin is a near theta solvent for polystyrene.[31] The polymer overlap concentration, c_p^*, was estimated from the standard equation

$$c_p^* = \frac{3M_w}{4\pi R_g^{\,3} N_A} \quad (1)$$

where $M_w = 18\,700$ g/mol is the molecular weight of the polymer, $R_g = 3.6$ nm is the polymer radius of gyration, and N_A is the Avogadro's number yielding $c_p^* = 0.16$ g/mL.

Phase diagram experiments for the depletion gels were performed in 10 mm o.d. Fisherbrand disposable culture tubes. The polymer solution of a given concentration was slowly added to a silica suspension of a given volume fraction until gelation was visually observed. For $\phi < 0.2$, the gels phase-separate into dense, amorphous colloidal sediment and a particle-free solution. For all the samples studied in this work, the problem of settling was not encountered during the time the rheological measurements were made.

Rheological measurements for the depletion systems were performed in the gel region. The polymer concentration was kept constant, and the rheological properties were measured as a function of colloid volume fraction. The procedure was repeated for different polymer concentrations: $c_p/c_p^* = 0.15$ (near the gel boundary), 0.2, 0.3, and 0.6 (deep inside the gel). All rheological data were gathered on a Bohlin C-VOR digital rheometer equipped with a cone and plate geometry (40 mm diameter, 4° cone angle, and 0.15 mm gap). Temperature control was maintained at 25 ± 0.1 °C with a CP-180 rapid Peltier temperature control module. Prior to the samples being loaded in the rheometer, the suspensions are homogenized. The suspension is then rapidly loaded into the measurement geometry, presheared at 450−600 s^{-1} for 180 s, and then allowed to reach a mechanical equilibrium state as determined by measurements of the time-dependent elastic modulus $G'(t)$ at a fixed oscillatory frequency of 1 Hz. A solvent trap was used to prevent evaporation, thereby allowing samples to remain in the rheometer without any measurable change in the rheological properties for up to 5 h.

The phase diagram of thermal gels was measured rheologically. The gel temperature at a particular volume fraction was taken to be the temperature at which the elastic modulus just falls below the loss modulus. Rheological measurements for the thermal gels were performed using a constant-stress rheometer with a temperature control of ±0.2 °C fitted with a cup and bob geometry with a 14 mm bob diameter and fixed outer cup diameter of 15.4 mm yielding a tool gap of 0.7 mm. A known volume (3 mL) of the sample was loaded into the rheometer at room temperature where the samples are easily flowing fluids and cooled to the desired temperature of measurement and allowed to equilibrate. Measurements of the elastic modulus were then made (with and without preshear) at a fixed oscillatory frequency of 1 Hz until the system reaches a state of mechanical equilibrium, as shown by the plateau of the elastic modulus with time.

Small angle neutron scattering (SANS) experiments were carried out using the NG-3 spectrometer at the National Institute of Standards and Technology in Gaithersburg, MD. The scattering vector, q, ranged from 0.01 to 0.3 nm^{-1}. The shearing was carried out in concentric cylinder geometry with a gap of 0.25 mm, and the inner cylinder was cooled with a circulating temperature-controlled bath. The intensity of the scattered neutrons was measured using a position-sensitive detector, and the raw data corrected for background, detector efficiency, and empty cell scattering and placed on an absolute scale using standards supplied by NIST. The NIST data presented in this work has not been corrected for smearing.

Ultra-small-angle X-ray scattering (USAXS) experiments were conducted at the UNICAT facility on the 33-ID line, Advanced Photon Source (APS) facility at Argonne National Laboratory. Similar to the rheological measurements, structure measurements were made at a fixed polymer concentration and varying ϕ and then repeated for different c_p/c_p^*. Details of the instrumental setup are given elsewhere.[32] The instrument utilizes a Bonse−Hart camera using Si(111) optics with additional side-reflection stages enabling effective pinhole collimation where desmeared data are obtained. The beam is 0.4 mm vertical by 1.5 mm horizontal through which 2×10^{13} photons are incident at 10 keV with a wavelength $\lambda = 1.54$ Å. The instrument has a q range of 2×10^{-4}−2×10^{-1} $Å^{-1}$ with a resolution of $\Delta q = 2 \times 10^{-4}$ $Å^{-1}$. The scattered beam is analyzed by rotating a Si(111) channel-cut crystal and measured by a photodiode detector. The narrow wavelength resolution ($\Delta\lambda/\lambda = 1.5 \times 10^{-4}$) ensures wavelength smearing effects are insignificant. All samples were loaded in custom-made aluminum cell holders with a 1 mm beam path length, enclosed between two Kapton polyimide film windows. Gels were shear-melted prior to loading in cells to improve workability. Experiments were carried out with high angular resolution (approximately 600 points between $10^{-4} \le q(Å^{-1}) \le 10^{-1}$).

3. Results and Discussion

3.1. Phase Behavior. Addition of nonadsorbing polymer to a colloidal suspension induces attractions between the particles with strength dependent on c_p/c_p^* and range set by $2R_g/D$. For dense suspensions ($\phi > 0.2$) with $2R_g/D < 0.1$, the suspensions gel with increasing c_p/c_p^*. In this work, $2R_g/D = 0.078$. The phase diagram of the depletion system is shown in Figure 1a where the amount of polymer required to form a gel (in units of c_p/c_p^*) is plotted as a function of ϕ. As can be seen from Figure 1a, the gel boundary is relatively flat, with $(c_p/c_p^*)_{gel}$ decreasing from 0.18 at $\phi = 0.1$ to $(c_p/c_p^*)_{gel} = 0.07$ at $\phi = 0.42$. To compare the depletion gel boundary with the thermal gel boundary, one needs a measure of the strength and range of attraction between the particles in the two different systems. An estimate of the strength of attraction at contact ($\epsilon_{depletion}/kT$) for the depletion system can be obtained from the contact value of Aasakura−Oosawa potential[33] (AO) which is commonly used to describe depletion systems. The interaction energy for the AO potential, $u_{AO}(r)$, is given by

(28) Stober, W.; Fink, A.; Bohn, E. *J. Colloid Interface Sci.* **1968**, *26*, 62.

(29) Bogush, G. H.; Tracy, M. A.; Zukoski, C. F. *J. Non-Cryst. Solids* **1988**, *104*, 95.

(30) Van Helden, A. K.; Jansen, J. W.; Vrij, A. *J. Colloid Interface Sci.* **1981**, *81*, 354.

(31) Shah, S. A.; Chen, Y. L.; Schweizer, K. S.; Zukoski, C. F. *J. Chem. Phys.* **2003**, *118*, 3350.

(32) Ilavsky, J.; Allen, A.; Long, G.; Jemian, P. *Rev. Sci. Inst.* **2002**, *73*, 1660.

$$\frac{u_{AO}(r)}{kT} = \begin{cases} \infty & \text{for } r < D \\ -\dfrac{c_p}{\alpha c_p^*}\left(1+\dfrac{D}{2R_g}\right)^3\left(1-\dfrac{3(2r/D)}{4^*(1+2R_g/D)}+\dfrac{(2r/D)^3}{16^*(1+2R_g/D)^3}\right) & \text{for } D < r < 1+2R_g/D \\ 0 & \text{for } r > 1+2R_g/D \end{cases} \quad (2)$$

where α is the polymer free-volume fraction.[34] The value of the AO potential at contact, $u_{AO}(r = D)$ is given by

$$\frac{u_{AO}(r=D)}{kT} = \frac{\epsilon_{depletion}}{kT} = -\frac{3}{2}\frac{D}{2R_g}\left(\frac{c_p}{c_p^*}\right)\frac{1}{\alpha} \quad (3)$$

Figure 2 is the phase diagram 1a replotted using the above eq 3 to give an estimate of the strength of attraction upon gelation in depletion systems. The range of interaction of the effective square well potential which gives rise to the gel boundary observed in Figure 1a with the strength of attraction at contact given by eq 3 can be determined by matching the second virial coefficient (B_2) of the AO and square well potential. The second virial coefficient for a given interaction energy $u(r)/kT$ is given by the following expression

$$B_2(T) = -2\pi \int_0^\infty [e^{-u(r)/kT} - 1]r^2\, dr \quad (4)$$

For a square well potential with strength of attraction at contact of ϵ and range Δ defined by

$$\frac{u_{SQ}(r)}{kT} = \begin{cases} \infty & \text{for } r < D \\ \epsilon/kT & \text{for } D < r < D(1+\Delta) \\ 0 & \text{for } r > D(1+\Delta) \end{cases} \quad (5)$$

the second virial coefficient defined by eq 4 reduces to

$$B_{2SQ}(T) = \frac{2\pi D^3}{3}[1 + \{(1+\Delta)^3 - 1\}(1 - e^{-\epsilon/kT})] \quad (6)$$

The effective square well width for the depletion gels is found by equating $B_{2AO} = B_{2SQ}$ at the same strengths of attraction at contact. On doing this for all values of c_p/c_p^* along the gel line in Figure 1a, we find the average well width $\Delta/D = 0.007$.

When suspended in decalin, the octadecyl silica particles behave as hard spheres at a room temperature of 25 °C. Reduction in temperature leads to decalin becoming a poor solvent for the octadecanol hairs and hence results in a temperature-induced attraction between the colloidal particles.[35] At a particular temperature, the particles are localized and the resulting gel has a finite elastic modulus. The phase diagram of this system is shown in Figure 1b for different volume fractions. The gel line is relatively flat with $T_{gel} = 1$ °C at $\phi = 0.1$ and $T_{gel} = 7$ °C at $\phi = 0.45$.

In the case of thermal gels, Jansen et al.[35] developed a square well model to describe the interactions between the octadecyl-coated silica particles suspended in different solvents. Flory−Krigbaum theory was used to predict the strength of attraction, $\epsilon_{thermal}$, at contact

$$\frac{\epsilon_{thermal}}{kT} = -A\left(\frac{T_\theta}{T} - 1\right) \text{ for } T \le T_\theta \quad (7)$$

where A is a factor proportional to the overlapping volume of the chains and T_θ is theta temperature of the chain solvent pair. The range of interaction in these systems, $\Delta_{thermal}$, is determined by the interpenetration distance between the octadecyl chains. The interpenetration distance is small[35] since the octadecyl chains are densely packed on the particle surface. In this work, we choose $\Delta_{thermal} = 1$ nm, yielding $\Delta_{thermal}/D = 0.01$.

Bergenholtz and Fuchs[19,20] developed a dynamic self-consistent mode coupling theory (MCT) to treat physical gelation of spherical particles interacting via a hard core repulsion plus short-range square well attraction. For short ranges of attraction ($\Delta/D \ll 1$) and low ϕ, a simple analytic expression was derived for the gel boundary linking the strength of attraction $(\epsilon/kT)_{gel}$ and volume fraction at gelation, ϕ_{gel}, as

$$\frac{12}{\pi^2}\frac{\Delta}{D}\phi_{gel}[\exp(-[\epsilon/kT]_{gel}) - 1]^2 = 1.42 \quad (8)$$

The gel boundary corresponding to eq 8 with $\Delta/D = 0.01$ is shown in Figure 2, indicating the ability of the simple expression to capture the location of gel boundaries in depletion systems. Substituting eq 7 into eq 8 and use

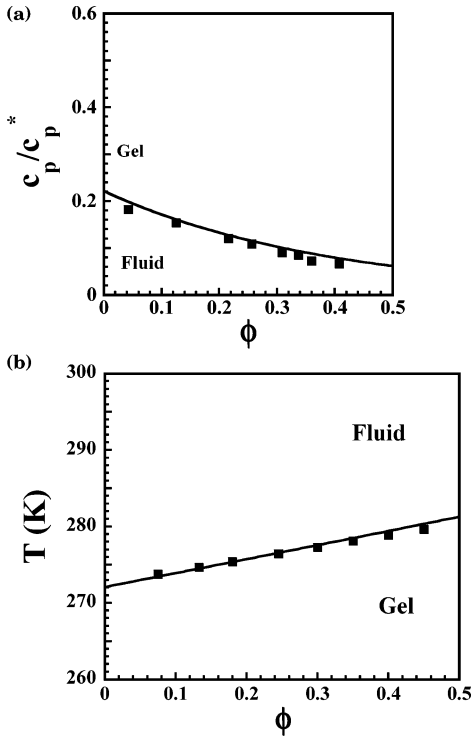

Figure 1. (a) Gel boundary (polymer concentration, c_p/c_p^*, vs colloid volume fraction, ϕ) of the octadecyl silica system in decalin upon addition of nonadsorbing polystyrene ($2R_g/D = 0.078$). The solid squares are the experimental points, while the solid line is a calculation of the gel boundary using eqs 3 and 8 with a width of interaction, Δ/D, of 0.007. The suspension is a fluid below the line, and as the polymer concentration increases and crosses the boundary, the system gels. (b) Gel boundary of octadecyl silica particles suspended in decalin upon reduction of temperature. The solid squares are the experimental points while the solid line is drawn using eqs 7 and 8 with $\Delta/D = 0.01$, $A = 29.2$, and $T_\theta = 306.8$ K. The suspension is a fluid above the line, and as one decreases the temperature and crosses the boundary, the system gels.

(33) Asakura, S.; Oosawa, F. *J. Polym. Sci.* **1958**, *33*, 183.
(34) Lekkerkerker, H. N. W.; Poon, W. C. K.; Pusey, P. N.; Stroobants, A.; Warren, P. B. *Europhys. Lett.* **1992**, *20*, 559.
(35) Jansen, J. W.; Dekruif, C. G.; Vrij, A. *J. Colloid Interface Sci.* **1986**, *114*, 471.

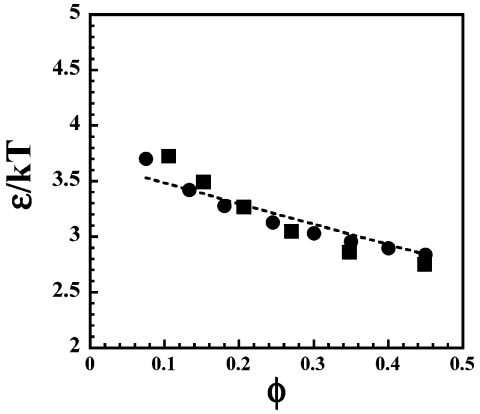

Figure 2. Strength of attraction at gelation for depletion (squares) and thermal gels (circles). Equation 3 is used for depletion gels, while eq 8 is used for thermal gels with $\Delta_{thermal}/D = 0.01$. The dashed line is a prediction of ϵ/kT by eq 7 with $A = 29.2$ and $T_\theta = 306.8$ K.

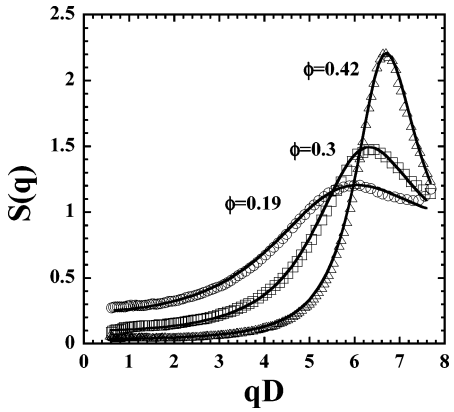

Figure 3. Structure factor ($S(q)$) of octadecyl silica suspensions suspended in decalin at $T = 25$ °C as measured by USAXS. The open symbols are experimental measurements at different volume fractions: $\phi = 0.19$ (circles), 0.3 (squares), and 0.42 (triangles). The solid lines are calculations of the hard sphere structure factor with Percus−Yevick closure.

of data in Figure 1b (thermal gel boundary) with $\Delta_{thermal}/D = 0.01$ yields $A = 29.2$ and $T_\theta = 306.8$ K. The dashed line in Figure 2 is the data points from the thermal gel replotted using eq 7 and the values of A and T_θ given above and illustrates the ability of these values to capture the gel behavior for the volume fraction range investigated.

As can be seen from Figure 2, the thermal and depletion gels which have similar ranges of attraction ($\Delta/D = 0.007$ and 0.01, respectively) gel at the same volume fractions at a given interaction energy. Since the gel boundaries are very similar, one would expect the elastic modulus of these different gels to be the same as one moves deeper into the gel by either increasing volume fraction or strength of attraction. Below, we explore the effect of moving along a line of fixed interaction energy by changing ϕ on the gel elastic modulus. In this way, we are able to explore the effects of gel microstructure on elastic modulus.

3.2. Quiescent Microstructure. The measured structure factor for the silica particles coated with octadecanol and suspended in decalin at 25 °C is shown in Figure 3. The open symbols are experimental points while the solid line is calculation of $S(q)$ for hard spheres using the Percus−Yevick closure. As can be seen from Figure 3, there is excellent agreement with experiment and theory suggesting the particles indeed behave as hard spheres. The low-q region is relatively flat, indicating the absence of clustering in hard sphere fluids even at high volume

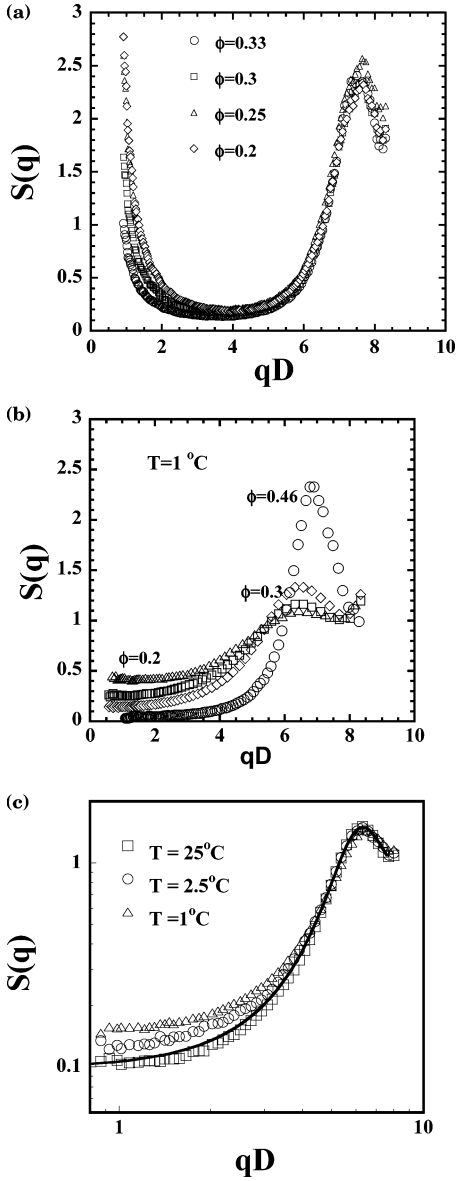

Figure 4. (a) Structure factor of depletion gels as measured by USAXS at c_p/c_p^* of 0.6 and at different volume fractions: $\phi = 0.2$ (diamonds), 0.25 (triangles), 0.3 (squares), and 0.33 (circles). The location of the first peak in the structure factor, q^*, and height of the first peak, $S(q^*)$, are invariant with colloid volume fraction. (b) Structure factor of thermal gels at 1 °C as measured by USAXS at different volume fractions: $\phi = 0.2$ (triangles), 0.25 (squares), 0.3 (diamonds), and 0.46 (circles). (c) Structure factor of thermal gel of $\phi = 0.3$ as measured by USAXS at different temperatures: $T = 25$ (squares), 2.5 (circles), and 1 °C (triangles). The solid line is a calculation of the hard sphere structure factor with Percus−Yevick closure at a ϕ of 0.3.

fractions. The location of the first peak in $S(q)-q^*$, which is a measure of the average spacing between the particles in the first cage shifts to higher wave vectors with increasing ϕ. This shift indicates that on average the particles move closer together as ϕ increases. The height of the first peak in $S(q)-S(q^*)$, a measure of the coherence of the first cage, increases with ϕ, and the increase seen in $S(q^*)$ with increasing ϕ is indicative of a tighter packing at higher ϕ. If the particles in the first cage have an FCC packing, q^*D would be approximately 7.8.

Figure 4a is a plot of structure factor $S(q)$ as measured by small-angle X-ray scattering for the depletion gels at a $c_p/c_p^* = 0.6$ at different volume fractions. The structure

factor is relatively insensitive to volume fraction variations in this range ($\phi \approx 0.2-0.4$) and also to the polymer concentration in the gel. Detailed discussions of the structure of depletion gels are given elsewhere,[26] and a brief summary of the key points follows. Depletion attractions induce structural reorganizations on three different length scales: (i) strong enhancement of local cage correlations and freezing in of the location and height of the first peak in structure factor with ϕ and c_p/c_p^*, (ii) suppression of intermediate length scale fluctuations (decreased osmotic compressibility), and (iii) a large amplitude, Porod-like upturn in $S(q)$ at small wavevectors. In accord with confocal microscopy results,[36] these features imply the emergence of dense, nonfractal clusters and narrow, random interfaces which are likely due to an annealing or compaction process on the depletion attraction scale $R_g \ll D$. The generic Debye−Bueche (D−B) model for randomly distributed heterogeneities is then used to analyze the low-q structure factor data and to back out an average correlation length between voids or heterogeneities which is expected to be closely related to a typical dense cluster size. From the D−B analysis, a cluster size of $\sim 3-4D$ is determined for the depletion gels and this cluster size is found to be insensitive to both ϕ and c_p/c_p^*. q^* and $S(q^*)$ are fixed at 7.8 and 2.5, respectively, indicative of dense packing within the clusters.

Figure 4b is a plot of the microstructure of the thermal gels at 1 °C at four different volume fractions. The structure of the thermal gels, as one can see, is very different from that of the depletion gels. There are no upturns at low q, and the height and location of the first peak shifts to higher wave vectors with increasing ϕ. The absence of upturns at low q indicates a lack of clustering in these gels. Changes in $S(q)$ with decreasing T at $\phi = 0.3$ is shown in Figure 4c. As T decreases from 25 °C where the particles are hard spheres to 1 °C, there is an increase in $S(0)$ while q^* and $S(q^*)$ hardly change from the hard sphere value. The increase in $S(0)$ with decreasing T is indicative of growth in weak attractions that result in long wavelength density fluctuations. These attractions do not cause clustering as seen in the low-q data of $S(q)$. The lack of change in q^* and $S(q^*)$ indicates that the average spacing of the particles in the first cage and the coherence are unaffected upon gelation. Thus, while the particles are freely diffusing in a liquid, gels occur when the particles become localized or "stuck" by changing their relative positions by a small distance compared to the hard sphere values. The origin of the difference in microstructure of the thermal gels from that of the depletion gels can possibly be due to a difference in the nature of the interaction potential. Depletion gels are a three-component system where the added polymers occupy space and if their entropy were to be maximized in the gel, the particles need to be pushed into clusters. The thermal gels are only a two-component system (colloid + solvent) in which the extra space available to the colloid due to the absence of polymer does not necessitate clustering.

3.3. Microstructure under Shear. The depletion gels used in this work are formed by high-shear mixing of the hard sphere and the polymer solution, while there is no shear involved in the formation of the thermal gels. Hence, one might suspect that, if the thermal gels were subjected to high shear, the particles would be pushed into clusters. Figure 5a is a plot of measured intensity as a function of qD for the thermal gel at a ϕ of 0.46 and at 1 °C under three different conditions: at rest, under shear at 1000 s^{-1}, and immediately after shear is stopped. The scattering under shear produces an anisotropic scattering pattern for both thermal and depletion gels. A simple circular integration of the scattering data is presented in Figure 5a and b to illustrate the formation (thermal gels) or breakup (depletion gels) of clusters. No quantitative information is extracted from these scattering curves.

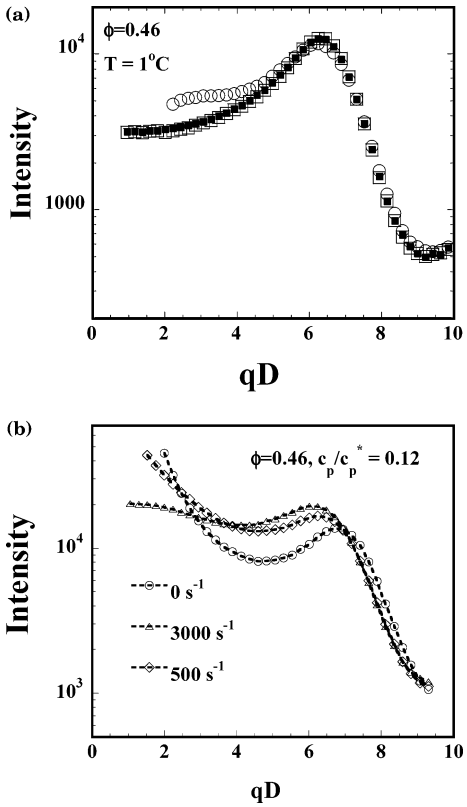

Figure 5. (a) Intensity as a function of qD for thermal gels as measured by SANS at $\phi = 0.46$ and $T = 1$ °C. The open squares are measured after quenching the sample to 1 °C with no applied shear. The open circles are experimental measurements when the sample is being sheared at a rate of 1000 s^{-1}. The solid squares represent the measured intensity immediately after shear is turned off. (b) Intensity as a function of qD for the depletion gel with $\phi = 0.46$ and $c_p/c_p^* = 0.12$ at different shear rates as measured by SANS: 0 (circles), 500 (diamonds), and 3000 s^{-1} (triangles). The dashed lines are drawn as a guide to the eye. The measured intensity after shear is turned off is identical to the 0 s^{-1} curve shown above.

As can been seen from Figure 5a, shear enhances scattering at low q, indicating shear-induced clustering in thermal gels. However, upon cessation of shear, the structure quickly relaxes back to the value at rest. This implies that the clusters that are formed under shear fall apart after shear is stopped. The behavior that is seen in Figure 5a is representative of all the thermal gels used in this work.

Figure 5b is a plot of measured intensity at rest and under two different shear rates for the depletion gel (500 and 3000 s^{-1}). Shear has the opposite effect on depletion gels than that of the thermal gels. Shear results in a suppression of scattering at low q, suggesting a breaking up of clusters of particles. However, as shear is turned off, the microstructure recovers back to that seen at rest and is identical to the 0 s^{-1} curve shown in Figure 5b.

The results presented above show that clusters are formed in depletion gels, upon addition of polymer to hard sphere suspensions. Clusters are not seen on quenching into the gel and clusters are not formed by shear. Thus, while we can map the location of the gel points to similar

(36) Varadan, P.; Solomon, M. J. *Langmuir* **2003**, *19*, 509.

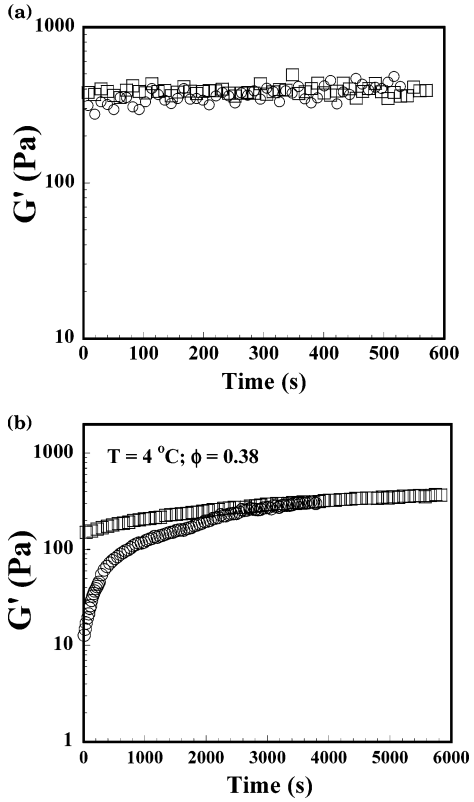

Figure 6. (a) Elastic modulus (G') as a function of time for the depletion gel with $\phi = 0.4$ and $c_p/c_p^* = 0.15$. The open squares are G' after the suspension has been sheared at 400 s^{-1} for 180 s and allowed to sit undisturbed for 30 min. The open circles show the modulus upon cessation of deformation at a shear rate of 400 s^{-1} for 180 s. The modulus recovers back to the plateau value almost instantaneously. (b) Elastic modulus (G') as a function of time for the thermal gel with $\phi = 0.38$ and $T = 4$ °C. The open circles are G' after cessation of shear (400 s^{-1} for 30 s), while the open squares are G' after the sample has been quenched to 4 °C and left undisturbed for an hour.

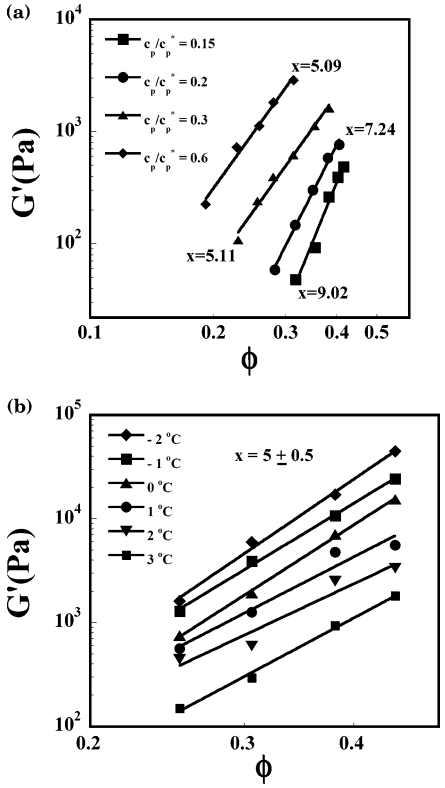

Figure 7. (a) Elastic modulus as a function of colloid volume fraction for depletion gels at different polymer concentrations $c_p/c_p^* = 0.6$ (diamonds), 0.3 (triangles), 0.2 (circles), and 0.15 (squares). The solid lines are power law fits to the elastic modulus $G' \sim \phi^x$ and the exponents x are given next to the respective experimental data. (b) Elastic modulus as a function of volume fraction, ϕ, for thermal gels at different temperatures. The solid lines are power law fits to the elastic modulus $G' \sim \phi^x$ and the exponent x is a constant at 5 ± 0.5 under all the conditions studied.

strength of attraction, the resulting materials have very different microstructures. If the composite model of Shah et al.[26] is correct, we anticipate that, at the same volume fraction and strength and extent of attraction, the modulus of the thermal gels will be substantially larger than the modulus of the depletion gels. Second, while shear alters the microstructures of both gels, as they relax back to structures identical to those seen before shear was initiated, we expect the modulus of both gel systems to recover to their presheared values upon cessation of shear.

3.4. Elastic Modulus. The elastic modulus of depletion gels at $\phi = 0.4$ and $c_p/c_p^* = 0.15$ as a function of time is shown in Figure 6a. The open squares are G' after the suspension has been sheared at 400 s^{-1} and allowed to sit undisturbed for 30 min. The open circles show the modulus as a function of time upon cessation of deformation at a shear rate of 400 s^{-1}. The modulus recovers to its rest value in a time frame shorter than that required to initiate measurements. In all the depletion gel samples studied in this work, recovery of G' was rapid and the time taken to recover was always on the order of a few minutes or less. A possible reason for this is that all the samples studied in this work are well inside the gel boundary. For samples near the gel boundary, Shah[37] reported that the time of recovery of G' can be of the order of 2−3 h. However, even in the samples studied by Shah, the value of G' immediately after shear is turned off is of order $0.9G'(t = \infty)$ and grows back to the plateau value, $G'(t = \infty)$. The data reported in Figure 6a are consistent with the neutron scattering data shown in Figure 5b. The recovery of G' mimics that of the structure in the sense that both structure and G' recover to the presheared state after cessation of shear.

The recovery of the modulus of thermal gels ($\phi = 0.38$ and $T = 4$ °C) is shown in Figure 6b. The squares represent the modulus of the as-quenched gel after an hour at the quench temperature. The open circles are the modulus after the suspension has been sheared at 400 s^{-1} for 30 s. The data shown in Figure 6b are again consistent with the neutron scattering data shown in Figure 5a in that both G' and $S(q)$ recover their quenched values after intense shear. The recovery times of the thermal gels are substantially longer than the depletion gels. G' starts from a low value (O(10 Pa)) after cessation of shear and slowly grows back to the plateau modulus before preshear. For samples close to the gel boundary and with a lower volume fraction, the recovery time is of the order of a few hours.

Parts a and b of Figure 7 are the elastic moduli of depletion and thermal gels, respectively, after they have recovered to a plateau value. The symbols are the experimental points, while the lines are power law fits to the elastic modulus. For both depletion and thermal gels, G' varies in a power law manner with exponent x ($G' \sim \phi^x$). However, x is different for the two different gels—x varies from 9 near the gel boundary to 5 deeper within the gel for depletion gels while it is a constant at a value of

(37) Shah, S. A.; Ph. D thesis, University of Illinois, 2004.

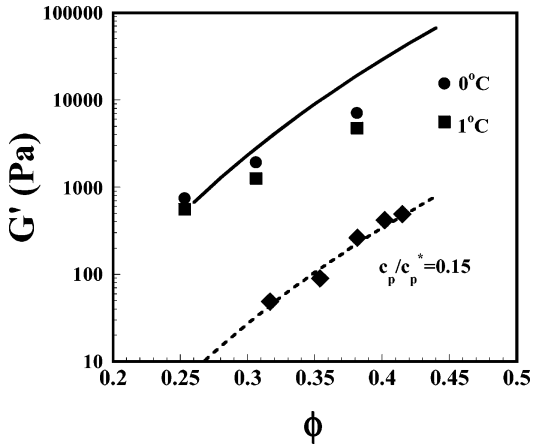

Figure 8. Elastic modulus as a function of volume fraction for depletion ($c_p/c_p^* = 0.15$, diamonds) and thermal gels ($T = 0$ °C, circles; 1 °C, squares). Moving along a path of constant $c_p/c_p^* = 0.15$ by increasing ϕ for depletion gels is equivalent to traversing a path in volume fraction with temperature between 0 and 1 °C for the thermal gels. The solid line is a calculation of G' for the depletion gel using NMCT. The dashed line is the theoretical calculation scaled by the number of particles in a cluster ($\sim 3-4D$). This comparison shows that at constant interaction energy, predictions of nonclustered depletion gels are close to those measured for thermal gels.

5 ± 0.5 for the thermal gels at all temperatures within the gel boundary. This is consistent with the study of Rueb and Zukoski[12] who observed similar exponents for the thermal gels of octadecyl silica particles in Decalin. The constant value of $x \approx 5$ for the thermal gels suggests that, relative to the depletion gels, attractions turn on very rapidly once the gel boundary is reached and small changes in T correspond to relatively small changes in c_p/c_p^*.

An important prediction of NMCT is that the length scale that controls the elastic modulus is r_{loc}, which is typically a small fraction of a particle diameter. Hence, G' would be dominated by the $q \approx 2\pi/r_{loc}$ or the high-q region of the $S(q)$ curve. This is validated by Figure 4c where there is hardly any change in the low-q region of $S(q)$ for a thermal gel of $\phi = 0.3$ when it is cooled from 25 °C (liquid) to 1 °C (a strong gel). The modulus of the sample at 1 °C is 1300 Pa. The differences between $S(q)$ at 25 °C and lower temperatures become smaller as volume fraction increases, while a stronger elastic modulus is observed at lower temperatures and higher ϕ's. These results suggest that structures on the length scale of a particle diameter and larger do not dominate gel mechanical properties.

To investigate the effect of clustering on G', a path along a line of constant interaction energy was followed by changing ϕ for both thermal and depletion gels. Theoretical calculations of interaction energies using the parameters given in the section on phase behavior show that moving along ϵ/kT of 3.5 is equivalent to moving along a c_p/c_p^* of 0.15 for depletion gels and keeping the temperature fixed between 0 and 1 °C for the thermal gels. Figure 8 is a plot of the measured elastic modulus for the depletion gels at a c_p/c_p^* of 0.15 and G' for thermal gels at 0 and 1 °C. The solid line shown in the plot is the calculation of G' at a c_p/c_p^* of 0.15 for the depletion gels using NMCT with the two-component PRISM as input for determining $S(q)$.[22,23] As discussed in previous studies,[13,23] the calculations of G' for the depletion gel are offset from the experimental measurements by the number of particles in the cluster which scales as the cube of the average cluster size. The average cluster size $\xi \approx 3-4D$ for depletion gels as measured by small-angle X-ray scattering. When the NMCT calculation is scaled by the number of particles in a cluster, there is excellent agreement between theory and experiment. Since there is no clustering present in the thermal gels, one would expect the predictions of NMCT to be of the same order of magnitude as the G' for thermal gels. As shown in Figure 8, NMCT calculations of G' for the depletion gels are indeed of the same magnitude as the thermal gels. In making this comparison, one should keep in mind that the depletion potential used in the NMCT calculation is a volume-fraction-dependent potential and involves two components (colloid and polymer). The square well potential used to model thermal gels is volume fraction independent and is an effective one-component interaction potential. Comparisons of elastic modulus of thermal gels with NMCT calculations with $S(q)$ calculated from a one-component attractive potential as input (square well or Yukawa potentials) is the subject of future study.

The agreement between NMCT predictions of gel elastic modulus and the thermal gels suggests several things. First, in agreement with previous studies, the presence of clusters reduces the modulus of the depletion gels and because the cluster size is independent of c_p/c_p^* and ϕ, when adjusted by a constant parameter of $(3-4D)^3$, model predictions and experiments are in near-quantitative agreement. Second, the thermal gels do not show the presence of clusters. As the particles in these gels experience an attraction with approximately the same extent, by working at approximately constant ϵ/kT, we find that the modulus predictions of NMCT for nonlcustered depletion gels are close to those measured for the thermal gels. These results suggest that the volume fraction dependencies of gel mechanical properties are dominated by density fluctuations of wave vector on the order of $2\pi/r_{loc}$ as opposed to $2\pi/D$ or smaller. The presence of the clusters in the depletion gels acts to reduce the gel modulus as expected for a composite material.

4. Summary and Conclusions

In this study, we have experimentally studied the microstructure and mechanical properties (elastic shear modulus) of depletion gels and thermal gels for different values of the strengths of interaction (c_p/c_p^* for depletion gels and temperature for thermal gels). Not all gels have the same microstructure—depletion gels are composed of dense clusters and voids while clustering is absent in thermal gels. The origin of dense clusters in depletion gels does not appear to be the result of shear. Shear breaks up clusters in depletion gels, which immediately form after shearing is stopped. In the case of thermal gels, shear produces clusters which break up after cessation of shear. The recovery of elastic modulus follows that of the structure in the sense that both structure and G' recover to the presheared state after cessation of shear. However, the recovery of modulus upon cessation of shear is not correlated with changes in microstructure on the order of $qD < 8$. Calculations of the gel boundary and elastic modulus performed by modeling the interactions with two-component PRISM (for depletion gels) and effective one-component square well model (for thermal gels) reveal that suspensions with interactions with similar extents of attraction gel at the same strength of attraction and have the same modulus for higher volume fractions—as long as the state of clustering in the gel is the same. Finally, in this paper we have developed a series of observations into a consistent picture for the behavior of colloidal gels. In doing this, we have tried to emulate the enthusiasm and rigor followed by Bob Rowell throughout his career as a scientist and editor.

Acknowledgment. This paper is written in honor of Bob Rowell who, over many years, has been a mentor and friend. We thank K. S. Schweizer for his insights and discussions. We thank P. R. Jemian (UNICAT) and L. Porcar (NIST) for their assistance in gathering the scattering data. The UNICAT facility at the Advanced Photon Source (APS) is supported by the U.S. DOE under Award No. DEFG02-91ER45439, through the Frederick Seitz Materials Research Laboratory at the University of Illinois at Urbana-Champaign, the Oak Ridge National Laboratory (U.S. DOE Contract No. DE-AC05-00OR22725 with UT-Battelle LLC), the National Institute of Standards and Technology (U.S. Department of Commerce), and UOP LLC. The APS is supported by the U.S. DOE, Basic Energy Sciences, Office of Science under Contract No. W-31-109-ENG-38. We acknowledge the support of the National Institute of Standards and Technology, U.S. Department of Commerce, in providing the neutron research facilities used in this work. This work utilized facilities supported in part by the National Science Foundation under Agreement No. DMR-9986442. Finally, we acknowledge financial support from the Nanoscale Science and Engineering Initiative of the National Science Foundation under NSF Award No. DMR-0117792.

LA050830W